Large-eddy simulations of Hector the convector making the stratosphere wetter

Thibaut Dauhut, Jean-pierre Chaboureau, Juan Escobar, Patrick Mascart

ATMOSPHERIC SCIENCE LETTERS
Atmos. Sci. Let. **16**: 135–140 (2015)
Published online 12 September 2014 in Wiley Online Library
(wileyonlinelibrary.com) **DOI:** 10.1002/asl2.534

RMetS
Royal Meteorological Society

Large-eddy simulations of Hector the convector making the stratosphere wetter

Thibaut Dauhut, Jean-Pierre Chaboureau,* Juan Escobar and Patrick Mascart

Laboratoire d'Aérologie, Université de Toulouse and CNRS, Observatoire Midi-Pyrénées, 14, avenue Edouard Belin 31400, France

**Correspondence to: J.-P. Chaboureau, Laboratoire d'Aérologie, Université de Toulouse and CNRS, Observatoire Midi-Pyrénées, 14, avenue Edouard Belin, 31400, France.*
E-mail: Jean-Pierre.Chaboureau@aero.obs-mip.fr

Received: 9 September 2013
Revised: 17 July 2014
Accepted: 19 August 2014

Abstract

A large-eddy simulation (LES) was performed for a Hector thunderstorm observed on 30 November 2005 over the Tiwi Islands. On that day, ice particles reaching 19-km altitude were measured. The LES developed overshooting updrafts penetrating the stratosphere that compared well with observations. Much of the water injected in the form of ice particles sublimated in the lower stratosphere. Net hydration was found with a 16% increase in water vapour. While moistening appeared to be robust with respect to the grid spacing used, grid spacing on the order of 100 m may be necessary for a reliable estimate of hydration.

Keywords: **tropical tropopause layer; large-eddy simulation; deep convection**

1. Introduction

The impact of tropical convection on the exchange between troposphere and stratosphere has long been considered negligible as thunderstorms only rarely reach heights exceeding 18 km. This supposed lack of rapid transfers of water and chemical components is simulated by existing climate models using horizontal grid spacings of 100 km or coarser. However, none of these models are able to explain the trends in stratospheric water vapour measured between 1950 and 2000 (e.g. Garcia *et al.,* 2007) or even the cooling trend in the upper tropical troposphere (Cordero, 2006). However, particles of ice and humid air pockets have been observed around convective systems in the lower tropical stratosphere in Brazil (Chaboureau *et al.,* 2007; Corti *et al.,* 2008), West Africa (Khaykin *et al.,* 2009) and Australia (Corti *et al.,* 2008). Associated numerical studies with more detailed models run with kilometre grid spacing showed that the tropical convection could extend above the local tropopause and enter the lower stratosphere up to an altitude 20 km (Chaboureau *et al.,* 2007; Grosvenor *et al.,* 2007; Chemel *et al.,* 2009). These studies support the idea that very deep convection can hydrate the stratosphere. However, the importance of the influence of transport by deep convection on the composition of the air in the upper troposphere and lower stratosphere remains an open and much debated question (e.g. Pommereau *et al.,* 2011).

Until now, numerical simulations of intense tropical storms reaching the lower stratosphere have most often been performed with a horizontal grid spacing of the order of 1 km. Because this resolution allows an explicit treatment of the convection, the models using such grid spacing are called cloud-resolving models (CRMs) or nowadays convection-permitting models. However, the representation of motion within the clouds remains insufficiently resolved. In particular, the effect of sub-cloud scale eddies is assumed to be accounted for the subgrid turbulence parameterization. This makes the convective transport estimated from these simulations uncertain. Several studies (e.g. Bryan *et al.,* 2003; Petch, 2006) have thus advocated the use of grid spacing of the order of 100 m to represent the convective flow correctly. With such a grid spacing, eddies that contain most of the kinetic energy are resolved in the so-called large-eddy simulation (LES) while small eddies that carry negligible flux are subgrid processes.

The objective of this study is to explore the sensitivity of convective water transport in the tropical stratosphere to the horizontal resolution in the range generally used by CRM and LES. The finest resolution employed here is the cubic grid spacing of 100 m, making it the world's first explicit simulation of convective transport and turbulence associated with a storm reaching the lower stratosphere. The thunderstorm studied is Hector, a storm that grew daily during pre-monsoon on the Tiwi Islands north of Darwin, Australia. A convective plume rising through the tropopause was observed over Hector by lidar on board the aircraft Geophysica flying more than 18 km above (Corti *et al.,* 2008). A series of simulations were performed with horizontal grid spacings of 1600, 800, 400, 200 and 100 m. They all successfully simulated the thunderstorm during its full life cycle, from its genesis to its dissipation.

2. Model and numerical experiments

The simulations were run with the Meso-NH model (Lafore *et al.,* 1998) on a domain centred over the Tiwi

islands. Recent development in the large parallel computing capability of Meso-NH (Pantillon *et al.,* 2011) made possible to run the model with 16 384 cores in LES mode over a large domain (2560 × 2048 × 256 gridpoints or 1.34 billion total grid points), wide enough not to be affected by the open lateral boundary conditions. The grid spacing of 100 m allowed the model to resolve the convection explicitly. The model top was set to 25 km with the upper 3 km including a sponge layer to damp gravity waves generated by the convection. The model used parameterizations for turbulence (Cuxart *et al.,* 2000), mixed-phase clouds (Pinty and Jabouille, 1998), and surface–atmosphere exchanges (Noilhan and Planton, 1989) and the radiative scheme used at ECMWF (Gregory *et al.,* 2000). The LES run was compared to simulations performed with the same parameterizations over the same domain of 256 × 204.8 km, but with coarser horizontal grid spacing of 1600, 800, 400 and 200 m. The simulations were integrated for 10 h.

The model was initialized by the sounding launched from Darwin at 0000 UTC 30 November 2005 (i.e. 0930 LST) characterized by a convective available potential energy of 2074 J kg^{-1}. Between 13 and 17 km, the water vapour content was taken from the European Centre for Medium-Range Weather Forecasts (ECMWF) analysis. Aloft, it was derived from the observations of Corti *et al.* (2008) with a linear increase from 2 ppmv at 380 K (∼17 km) to 4 ppmv at 410 K (∼18 km) and a 4 ppmv value aloft. No large-scale forcing was applied. Information on orography and land cover is obtained from 1-km resolution databases ensuring that the same surface description was applied for the simulations with horizontal grid spacing ranging from 100- to 800-m. Surface conditions were taken from the ECMWF analysis with a sea surface temperature of 302 K, a surface soil temperature of 303 K and a moisture content of 0.16 m^3 m^{-3}. Convection was triggered as the result of the sea breeze induced by the contrasting surface latent and sensible heat fluxes over land and sea. Outputs from the simulations were averaged over a rectangular domain of 173.2 × 93.2 km centred on the Tiwi islands and were saved every 5 min.

3. Results

Figure 1(a) shows a vertical section of total water across Hector at 1400 LST during its most intense phase in the LES. On the left, the storm cell dissipates leaving a wet pocket in the stratosphere. On the right, the cell is fully developed vertically. Its cloud envelope reaches the tropopause located 17 km away and a plume of condensed water is injected above an altitude of 19 km. Because of the rapid upward motion, the right-hand cell is upright and full of cloud particles in an unchanged background of water vapour. Figure 1(b) zooms in on some details of the left-hand plume. It displays a 15-km wide convective core at the tropopause. Aloft, the plume is characterized by a residual cloud a few hundred metres high surrounded by positive anomalies of water vapour stretched by the shear of the stratospheric winds.

The dissipating plume shares some characteristics with what was observed from the stratospheric aircraft (Corti *et al.,* 2008). Figure 1(c) shows the backscatter ratio from lidar observations during 400 s, which corresponds to a distance of 80 km given a flight speed of 200 m s^{-1}. The convective core is also about 15-km wide at the tropopause. A straight plume reached 18 km altitude while cloud remnants are spread with the winds (note that the Geophysica aircraft did not have a straight flight path). A 15-ppmv maximum of total water was measured at the aircraft altitude, which was attributed to ice particles (Corti *et al.,* 2008). This maximum value roughly corresponds to the in-cloud values associated with the left-hand cell in the simulation. The observed maximum is however much lower than the values simulated in the right-hand cell shown in Figure 1(a). The aircraft measurement was made at 1620 LST, 20 min after the end of the convective episode (Chemel *et al.,* 2009).

Figure 2 shows the water vapour content at 18 km altitude in the LES. At 1400 LST, some pockets of moist air are located in the vicinity of the convective towers shown in Figure 1(a). Some of them are organized as rings around eyes of unchanged water contents, which are the imprints of convective plumes overshooting the altitude of 18 km. The other pockets of moist air were created by convective plumes reaching 18 km altitude at most. At 1800 LST, the storm activity had been over for 2 h. In the lower stratosphere, turbulent motions generated by convective updrafts had dissipated leaving a water vapour content fluctuating around 4 ppmv over the main island. A 50-km long pocket of moist air was located over the western coast of the Tiwi islands. This residual anomaly was transported westward away from the convective sources by the winds aloft. It reached water vapour values between 6 and 9 ppmv.

Because the main driving force of stratospheric hydration by Hector is the strength of the updrafts that carry water, we now compare the updraft intensity and hydrometeor content as well as cloud fraction and entrainment (calculated below freezing level using the standard bulk plume model) among the five simulations. Updrafts were defined as grid points where vertical wind speed exceeds 1 m s^{-1}. The distributions shown in Figure 3 were analysed between 1330 and 1530 LST and over a rectangular domain encompassing the Tiwi islands. In the boundary layer, the entrainment is dominated by the many small clouds. As expected, it is reduced with coarser resolution as small clouds are less resolved (thus less numerous). The reduced entrainment into the base of the updrafts makes them weaker at coarser resolution. As a result, the vertical velocity for the most rapid updrafts generally decreases with reduced resolution. The change in updraft properties at the cloud base with resolution has an impact on the vertical development of the convection up to the lower stratosphere. The strong updrafts in the boundary layer obtained by the three finest simulations reinforce the

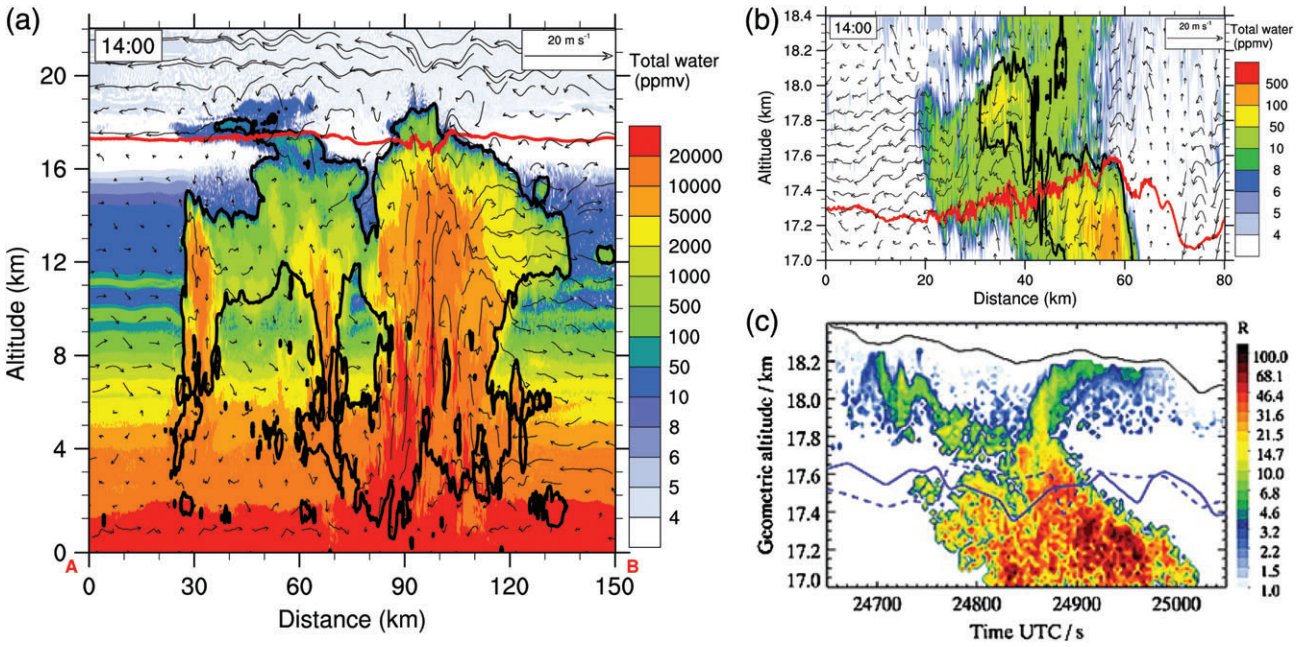

Figure 1. (a) Vertical section of total water across Hector on 30 November 2005 at 1400 LST along the line AB show in Figure 2. (b) Zoom on the upper part of (a). (c) Backscatter ratio from lidar observation; figure taken from Corti *et al.* (2008). The 380-K isentrope is represented by a red line in (a) and (b), and a blue line in (c). The black line delineates the cloud limit with condensed water mixing ratio larger than 10^{-5} kg kg^{-1} in (a) and (b) and the aircraft altitude in (c).

updrafts in the upper troposphere. The weaker updrafts produced in the boundary layer by the 1600-m simulation yield a larger cloud fraction and lower hydrometeor content in the free troposphere. This sensitivity of the updraft hydrometeor content to resolution is clearly seen above the freezing level and is the most dramatic for the 99th percentile updraft quantities. Around 17 km, the updraft hydrometeor content values decrease strongly reaching zero values at 19-km altitude. Above that level, upward wind velocities are due to gravity waves. Note that the 400-m simulation produces the highest vertical velocity. This is due to an underestimation of mixing in the boundary layer by the turbulence scheme (Honnert *et al.,* 2011). Such a drawback is a common modelling issue for grid spacing ranging between the mesoscale and LES limits, Wyngaard's so-called terra incognita. It is worth noting that near-convergence in the quantities shown in Figure 3 is obtained for the LES and the 200-m simulation.

Total water and water vapour were averaged every 5 min over the same rectangular domain as used to analyse updraft properties and in the layer between the tropopause and the maximum altitude reached by the convective plume, that is between 17- and 20-km altitude. The time evolution of water was similar among the simulations (Figure 4). All the simulations showed an abrupt increase in total water at 1300 LST that lasted about 1 h (at the exception of the 1600-m simulation for which convection started about 1 h earlier.) This short duration corresponds to the period of intense convection, which has been observed by radar (Chemel *et al.,* 2009). From 1400 LST onwards the total water decreased mostly due to hydrometeors precipitating below the 17 km altitude. From that time, the water vapour increased from an average value of 3.7–4.3 ppmv at 1600 LST. Because the low temperature at the tropopause (188 K) limited the export of water vapour from the troposphere, the increase in water vapour was explained by ice crystals sublimating before they could reach the troposphere back. At 1830 LST the total water in excess was in the form of vapour only. This air, enriched in water vapour, was then transported outside the domain encompassing the Tiwi islands by the easterlies.

The total water and water vapour content in the lower stratosphere changed with the resolution. The coarser-resolution simulations tended to develop more rapidly, which resulted in ice injection from 1200 LST onwards, compared with 1320 LST in the LES. Because the water vapour was produced from the ice particles, its increase was also delayed by 80 min in the LES. The maximum of total water varied between 10 and 33 ppmv with the grid spacings of 1600 and 400 m, respectively. However, the LES and the 200-m simulation showed a similar maximum of 13 ppmv. The variation in the water vapour content maximum was small between 4.2 and 4.7 ppmv. These values correspond to a net increase in water vapour between 12 and 27%. Again, the LES and the 200-m simulation showed good agreement with an increase of 16 and 18%, respectively.

When integrating over the domain encompassing the Tiwi islands, a net hydration of 2776 t was found for the LES (against 2222, 2252, 4525 and 3263 t for the 1600-, 800-, 400- and 200-m simulations, respectively). By averaging over potential temperature levels 380–420 K (~17–18.5 km), Chemel *et al.* (2009) found a moistening of 0.06 and 2.24 ppmv for the two models they run with a 1-km horizontal grid spacing.

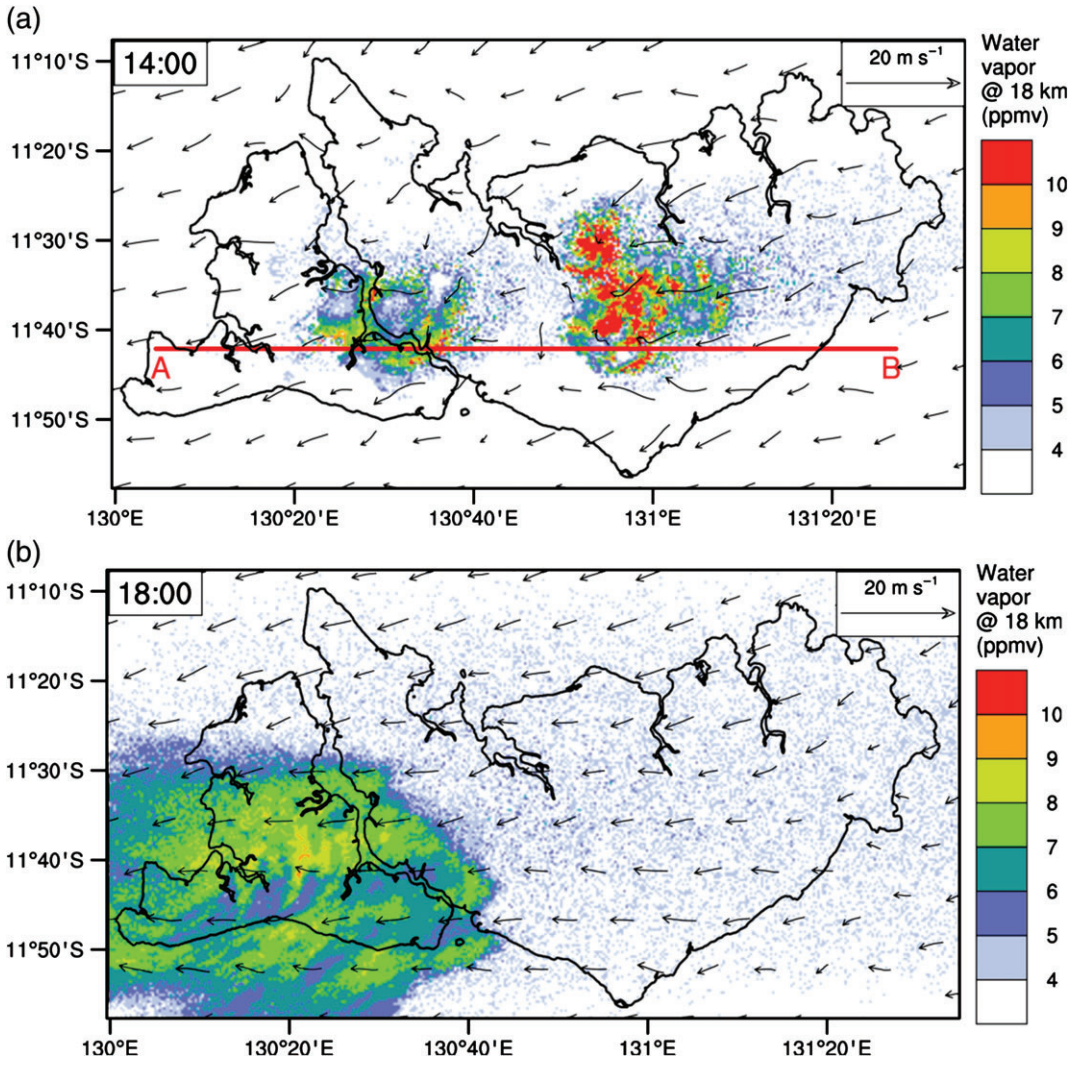

Figure 2. Water vapour mixing ratio (shading, ppmv) and horizontal wind (vector, m s^{-1}) at 18 km-altitude at (a) 1400 and (b) 1800 LST. In (a), the red line represents the position of the vertical cross section shown in Figure 1(a).

Integrated over their model domains and with an air density taken to be 0.165 kg m^{-3}, these increases corresponded to a net hydration of 1072 and 28 959 t, respectively. Thus, the estimates given here are in the range of those found by Chemel *et al.* (2009). However the range of uncertainty in the results of Chemel *et al.* (2009) is more than one order of magnitude. Further work, such as model intercomparison using the idealized set-up implemented here, is needed to reduce this strong uncertainty.

4. Concluding remarks

A LES of the storm Hector showed that it substantially hydrated the lower stratosphere by injecting ice particles, some of which sublimated into 2776 t of water vapour. As in simulations at coarser resolution, a moistening rather than a drying was robust with respect to the grid spacing. However, uncertainty on the water vapour content was high. It is worth mentioning that convergence on the import of water vapour into the stratosphere has still not been attained between the LES and the 200-m simulation. Nevertheless, these two simulations do agree on the water vapour increase within 20%.

These small scale processes should have an impact on a large scale. From the estimated value of 2776 t, the local impact of Hector can be scaled up to calculate the contribution of the convective overshoots to the annual mean upward water vapour flux across the 100 hPa level (2×10^9 kg day^{-1} according to Lelieveld *et al.* (2007)). On the basis of 5-year observations by the Tropical Rainfall Measuring Mission (TRMM) precipitation radar, 5512 tropical convection systems penetrated the 380-K potential temperature level (Liu and Zipser, 2005). Given a 50-day revisit time for TRMM, the contribution from convection would represent 18% of the total flux.

Of course this estimate needs to be appreciated with regard to the large uncertainties that are associated with all the figures given above. First, the local contribution of Hector found here is in the range of previous estimates but the degree of uncertainty on the

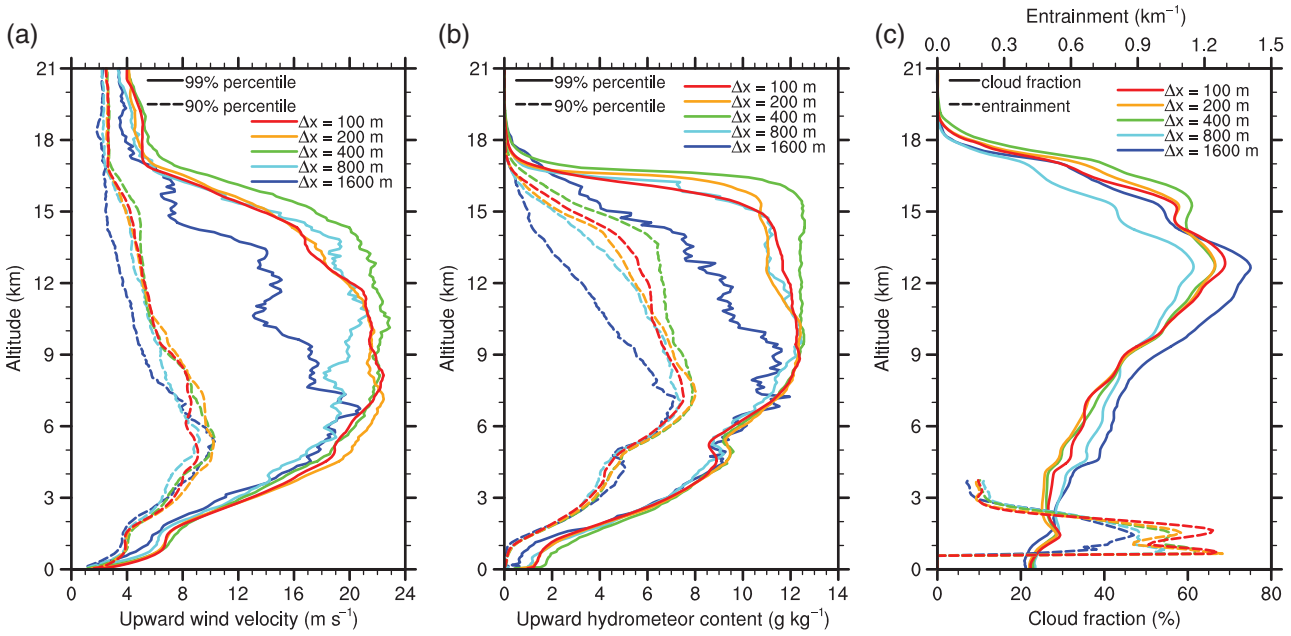

Figure 3. Vertical profiles of quantities obtained between 1330 and 1530 LST over the rectangular domain shown in Figure 2: 90th and 99th percentile upward (a) wind velocity and (b) hydrometeor content and (c) mean cloud fraction and entrainment (below freezing level).

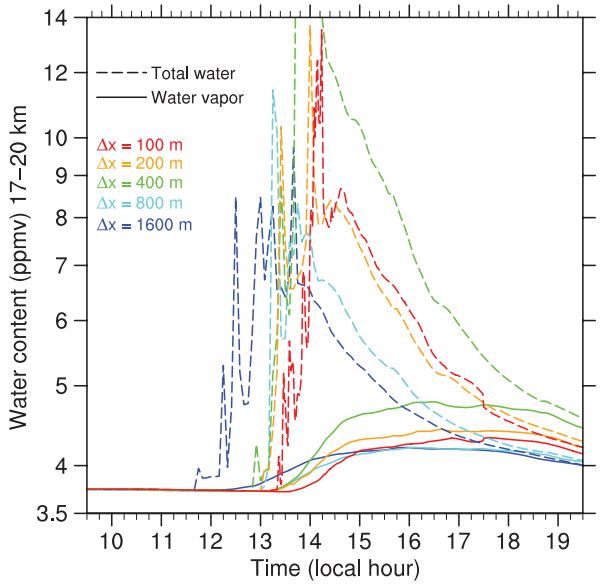

Figure 4. Total water (dashed line) and water vapour (solid line) mixing ratio averaged between 17 and 20 km altitude over the rectangular domain shown in Figure 2.

present results is larger than one order of magnitude. Second, the sensitivity to microphysics remains to be investigated as the microphysical processes are essential for controlling the water flux at the tropopause including the sublimation of ice into vapour and the change in buoyancy during phase transformation. An intercomparison between models running with a grid spacing of at least 200 m would allow to progress to be made on that point. Finally, the simulation of other storms in contrasting weather environments remains to be studied to assess the importance of the impact of convective transport on a global scale.

Acknowledgements

This research was supported by the CNRS/INSU LEFE MANGO project and StratoClim funded by the European Union Seventh Framework Programme under grant agreement no 603557. Computer resources were allocated by GENCI trough projects 90569 and 100231 (Grand Challenge Turing).

References

Bryan GH, Wyngaard JC, Fritsch JM. 2003. Resolution requirements for the simulation of deep moist convection. *Monthly Weather Review* **131**: 2394–2416, doi: 10.1175/1520-0493(2003)131<2394:RRFTSO>2.0.CO;2.

Chaboureau JP, Cammas JP, Duron J, Mascart PJ, Sitnikov NM, Voessing HJ. 2007. A numerical study of tropical cross-tropopause transport by convective overshoots. *Atmospheric Chemistry and Physics* **7**: 1731–1740, doi: 10.5194/acp-7-1731-2007.

Chemel C, Russo MR, Pyle JA, Sokhi RS, Schiller C. 2009. Quantifying the imprint of a severe Hector thunderstorm during ACTIVE/SCOUT-O3 onto the water content in the upper troposphere/lower stratosphere. *Monthly Weather Review* **137**: 2493–2514, doi: 10.1175/2008MWR2666.1.

Cordero EC, de F. Forster PM. 2006. Stratospheric variability and trends in models used for the IPCC AR4. *Atmospheric Chemistry and Physics* **6**: 5369–5380, doi: 10.5194/acp-6-5369-2006.

Corti T, Luo BP, de Reus M, Brunner D, Cairo F, Mahoney MJ, Martucci G, Matthey R, Mitev V, dos Santos FH, Schiller C, Shur G, Sitnikov NM, Spelten N, Vössing HJ, Borrmann S, Peter T. 2008. Unprecedented evidence for deep convection hydrating the tropical stratosphere. *Geophysical Research Letters* **35**: L10810, doi: 10.1029/2008GL033641.

Cuxart J, Bougeault P, Redelsperger JL. 2000. A turbulence scheme allowing for mesoscale and large-eddy simulations. *Quarterly Journal of Royal Meteorological Society* **126**: 1–30, doi: 10.1002/qj.49712656202.

Garcia RR, Marsh DR, Kinnison DE, Boville BA, Sassi F. 2007. Simulation of secular trends in the middle atmosphere, 1950–2003. *Journal of Geophysical Research* **112**, doi: 10.1029/2006JD007485.

Gregory D, Morcrette JJ, Jakob C, Beljaars AM, Stockdale T. 2000. Revision of convection, radiation and cloud schemes in the ECMWF

model. *Quarterly Journal of Royal Meteorological Society* **126**: 1685–1710, doi: 10.1002/qj.49712656607.

Grosvenor DP, Choularton TW, Coe H, Held G. 2007. A study of the effect of overshooting deep convection on the water content of the TTL and lower stratosphere from Cloud Resolving Model simulations. *Atmospheric Chemistry and Physics* **7**: 4977–5002, doi: 10.5194/acp-7-4977-2007.

Honnert R, Masson V, Couvreux F. 2011. A diagnostic for evaluating the representation of turbulence in atmospheric models at the kilometric scale. *Journal of the Atmospheric Sciences* **68**: 3112–3131.

Khaykin S, Pommereau J-P, Korshunov L, Yushkov V, Nielsen J, Larsen N, Christensen T, Garnier A, Lukyanov A, Williams E. 2009. Hydration of the lower stratosphere by ice crystal geysers over land convective systems. *Atmospheric Chemistry and Physics* **9**: 2275–2287, doi: 10.5194/acp-9-2275-2009.

Lafore JP, Stein J, Asencio N, Bougeault P, Ducrocq V, Duron J, Fischer C, Héreil P, Mascart P, Masson V, Pinty JP, Redelsperger JL, Richard E, Vilà-Guerau de Arellano J. 1998. The Meso-NH Atmospheric Simulation System. Part I: adiabatic formulation and control simulations. *Annals of Geophysics* **16**: 90–109, doi: 10.1007/s00585-997-0090-6.

Lelieveld J, Brühl C, Jöckel P, Steil B, Crutzen PJ, Fischer H, Giorgetta MA, Hoor P, Lawrence MG, Sausen R, Tost H. 2007. Stratospheric dryness: model simulations and satellite observations. *Atmospheric Chemistry and Physics* **7**: 1313–1332, doi: 10.5194/acp-7-1313-2007.

Liu C, Zipser EJ. 2005. Global distribution of convection penetrating the tropical tropopause. *Journal of Geophysical Research* **110**: D23104, doi: 10.1029/2005JD006063.

Noilhan J, Planton S. 1989. A simple parameterization of land surface processes for meteorological models. *Monthly Weather Review* **117**: 536–549, doi: 10.1175/1520-0493(1989)117<0536:ASPOLS>2.0.CO;2.

Pantillon F, Mascart P, Chaboureau JP, Lac C, Escobar J, Duron J. 2011. Seamless MESO-NH modeling over very large grids. *Comptes Rendus Mécanique* **339**: 136–140, doi: 10.1016/j.crme.2010.12.002.

Petch J. 2006. Sensitivity studies of developing convection in cloud-resolving model. *Quarterly Journal of Royal Meteorological Society* **132**: 345–358, doi: 10.1256/qj.05.71.

Pinty JP, Jabouille P. 1998. A mixed-phase cloud parameterization for use in a mesoscale non-hydrostatic model: simulations of a squall line and of orographic precipitations. In *Conference on Cloud Physics*. American Meteorological Society: Everett, WA; 217–220.

Pommereau JP, Garnier A, Held G, Gomes AM, Goutail F, Durry G, Borchi F, Hauchecorne A, Montoux N, Cocquerez P, Letrenne G, Vial F, Hertzog A, Legras B, Pisso I, Pyle JA, Harris NRP, Jones RL, Robinson AD, Hansford G, Eden L, Gardiner T, Swann N, Knudsen B, Larsen N, Nielsen JK, Christensen T, Cairo F, Fierli F, Pirre M, Marécal V, Huret N, Rivière ED, Coe H, Grosvenor D, Edvarsen K, Di Donfrancesco G, Ricaud P, Berthelier J-J, Godefroy M, Seran E, Longo K, Freitas S. 2011. An overview of the HIBISCUS campaign. *Atmospheric Chemistry and Physics* **11**: 2309–2339, doi: 10.5194/acp-11-2309-2011.